

Figure S1: Land use cover within the study area. Data obtained from GeodatenOnline, a service by the Bavarian State Office for Digitisation, High-Speed Internet and Surveying (Landesamt für Digitalisierung, Breitband und Vermessung, LDBV).

5

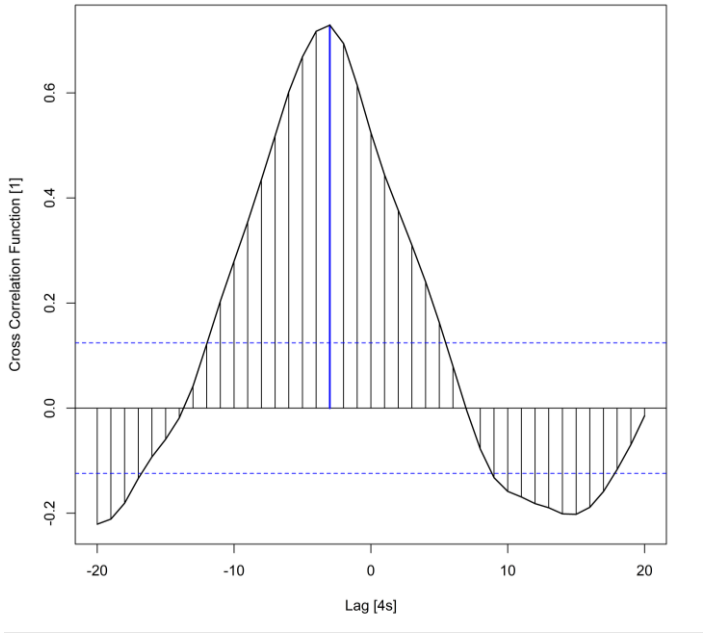


Figure S2: Cross-correlation of NO_2 against CO_2 to determine the inlet residence time for the NO_2 instrument. Horizontal dotted blue lines indicate the 95% confidence intervals, and the maximum of the cross-correlation function is marked with the vertical blue line.

Table S1: List of species identified but not calibrated with the PTR-ToF-MS. MVK+MACR = methyl vinyl ketone + methacrolein; MEK = methyl ethyl ketone.

Compound	Sum formula	[M] / g mol^{-1}	[M+H]$^+$ / m/z	Selected peak / m/z
Formaldehyde	CH_2O	30.03	31.0178	31.0149
Ethanol	C_2H_6O	46.07	47.0491	47.0483
Acrolein	C_3H_4O	56.06	57.0335	57.0332
Acetic acid	$C_2H_4O_2$	60.05	61.0284	61.0269
Dimethyl sulfide	C_2H_6S	62.13	63.0263	63.0251
Furan	C_4H_4O	68.07	69.0335	69.0315
MVK+MACR	C_4H_6O	70.09	71.0491	71.0475
Methylglyoxal	$C_3H_4O_2$	72.06	73.0284	73.0289
MEK	C_4H_8O	72.11	73.0648	73.0636
Phenol	C_6H_6O	94.11	95.0491	95.0474
Benzaldehyde	C_7H_6O	106.12	107.0491	107.0507
Cresols	C_7H_8O	108.14	109.0648	109.0659
Naphthalene	$C_{10}H_8$	128.17	129.0699	129.0704
Sesquiterpenes	$C_{15}H_{24}$	204.63	205.1951	205.1953
D4-Siloxane	$C_8H_{24}O_4Si_4$	296.62	297.0824	297.0858
D5-Siloxane	$C_{10}H_{30}O_5Si_5$	370.77	371.1012	371.1035

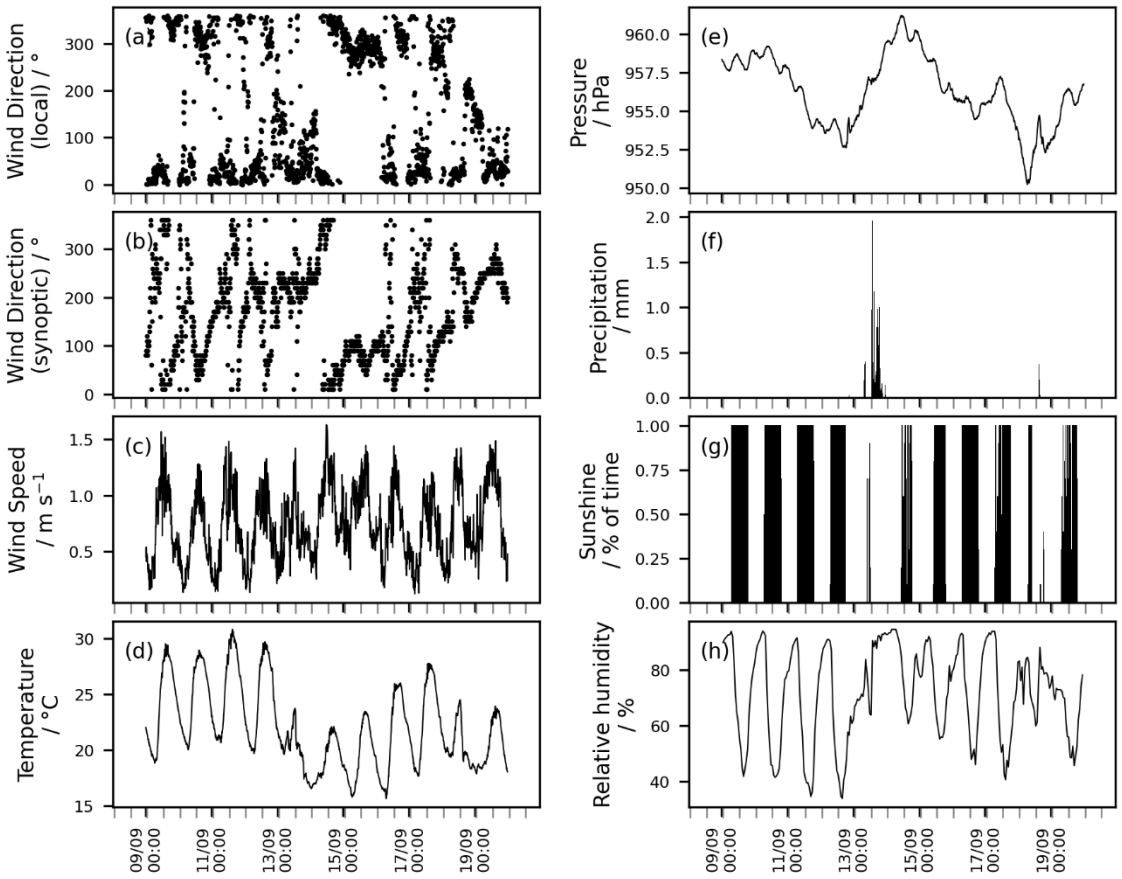


Figure S3: Meteorological conditions during the mobile measurements. Local wind direction, wind speed, temperature, and pressure were recorded with the instrumentation of the mobile laboratory. Synoptic wind direction, precipitation, sunshine, and relative humidity were accessed from the urban climate station München-Stadt (# 03379, 48.163202°N, 11.542893°E, approximately 300 m distance to Landshuter Allee) operated by the German weather service (Deutscher Wetterdienst, DWD). Precipitation (and sunshine) are sum values over 10-minute-intervals. The time is shown as the local time.

Table S2: List of all rides in the study area. R1 and R2 are the different routes (see Error! Reference source not found.**b).**

Date	Day of week	Ride	Local time	R1	R2
10/09/2023	Sunday	D1R1R1	17:00 – 17:53	2	0
11/09/2023	Monday	D2R2	11:58 – 12:10	0	1
		D2R1	19:40 – 19:55	1	0
12/09/2023	Tuesday	D3R2R1R2R1R2R1R2	11:00 – 13:16	3	4
		D3R1R2R1	18:20 – 19:20	2	1
14/09/2023	Thursday	D5R1R2R1R2	15:02 – 16:15	2	2
15/09/2023	Friday	D6R2R1R2R1R2R1R2R1R1	03:57 – 05:57	5	4
		D6R1R2R1R2R1R2R1	11:14 – 13:15	4	3
		D6R1R2R1R2	18:57 – 20:00	2	2
16/09/2023	Saturday	D7R2R1R2R1R2R1	13:09 – 14:39	3	3
17/09/2023	Sunday	D8R2R1R2R1R2R1	11:35 – 13:08	3	3
18/09/2023	Monday	D9R2R1R2R1R2R1R2	10:55 – 12:40	3	4
				∑ 30	∑ 27

Table S3: Reactivity and potential to form secondary pollutants of the measured compounds. Rate coefficients for the reactions with OH radicals, with O_3, and with NO_3 radicals are listed and apply to T = 298 K unless stated otherwise. If available, IUPAC-recommended values were used. Maximum incremental reactivities (MIR) and high-NO_x secondary organic aerosol yields (SOAy) are literature values (Carter, 2009; Gu et al., 2021; Wu and Xie, 2018). For NO and NO_2, only the rate coefficients for OH radical reactions are listed, as these were needed to calculate the NO_x OH reactivity to constrain the parameter θ for O_3 production sensitivity.

Compound	k(OH) / molecules^{-1} cm^3 s^{-1}	k(O_3) / molecules^{-1} cm^3 s^{-1}	k(NO_3) / molecules^{-1} cm^3 s^{-1}	MIR / g g^{-1}	SOAy / [-]
Methanol	9.0×10^{-13} (IUPAC, 2026)	n/a	1.3×10^{-16} (IUPAC, 2026)	0.67	0.00
Acetonitrile	2.2×10^{-14} (IUPAC, 2026)	n/a	n/a	n/a	n/a
Acetaldehyde	1.5×10^{-11} (IUPAC, 2026)	6.0×10^{-21} (Atkinson et al., 1981)[a,1]	2.7×10^{-15} (IUPAC, 2026)	6.54	0.00
Acetone	1.8×10^{-13} (IUPAC, 2026)	n/a	3.0×10^{-17} (IUPAC, 2026)[l]	0.36	0.01
Isoprene	1.0×10^{-10} (IUPAC, 2026)	1.28×10^{-17} (IUPAC, 2026)	6.5×10^{-13} (IUPAC, 2026)	10.61	0.01
Benzene	1.2×10^{-12} (IUPAC, 2026)	1.0×10^{-21} (IUPAC, 2026)[l]	3.0×10^{-17} (IUPAC, 2026)[l]	0.72	0.24
2-Methyl-2-Pentene	8.76×10^{-11} (Ohta, 1984)	4.54×10^{-16} (Duncianu et al., 2012)[b]	n/a	11.00	0.02
Toluene	5.6×10^{-12} (IUPAC, 2026)	1.0×10^{-21} (IUPAC, 2026)[l]	7.8×10^{-17} (IUPAC, 2026)	4.00	0.36
m-Xylene	2.2×10^{-11} (Kramp and Paulson, 1998)[a]	6.0×10^{-22} (Pate et al., 1976)[b]	7.1×10^{-17} (Atkinson et al., 1984)[a]	7.80	0.08
1,2,3-Trimethylbenzene	2.89×10^{-11} (Bohn and Zetzsch, 2012)	1.6×10^{-21} (Pate et al., 1976)[b]	5.6×10^{-16} (Atkinson et al., 1984)[a]	11.97	0.02
m-Diethylbenzene	2.2×10^{-11} (Shaw et al., 2020)[a]	n/a	n/a	7.10	0.06
α-Pinene	5.3×10^{-11} (IUPAC, 2026)	9.6×10^{-17} (IUPAC, 2026)	6.2×10^{-12} (IUPAC, 2026)	4.01	0.13
NO	9.7×10^{-12} (IUPAC, 2026)				
NO_2	1.12×10^{-11} (IUPAC, 2026)				

[(a)] at T = 296 K

[(b)] at T = 297 K

[(1)] upper limit

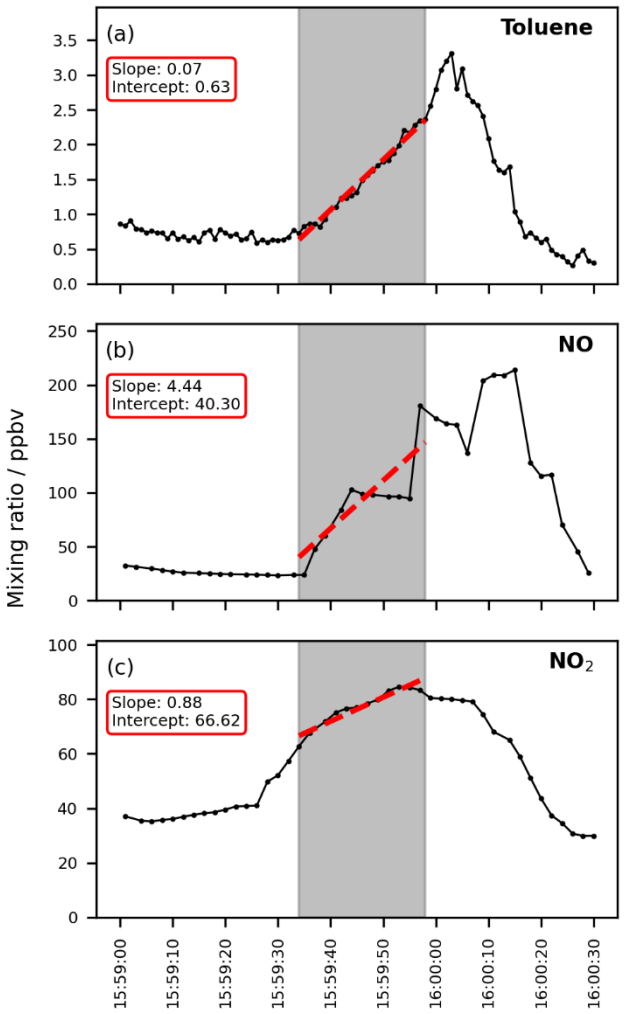


Figure S4: Time series of an exemplary ride through the tunnel (shaded in grey) during rush hour on the 14th of September, 2023 for (D5R1R2R1R2). The time is shown as the local time.

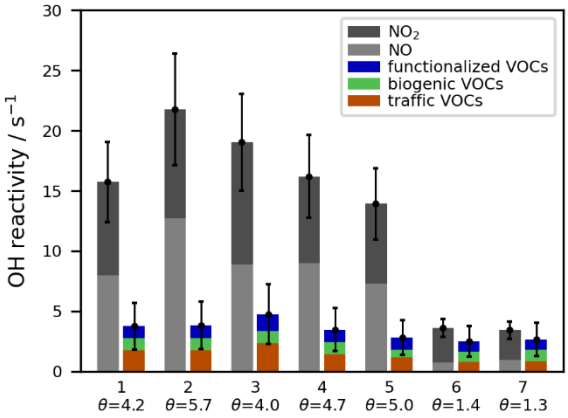


Figure S5: Comparison of NO_x OH reactivity and VOC OH reactivity for the focus areas. Error bars show the total error for either the NO_x OH reactivity or the VOC OH reactivity, calculated from the propagation of assumed uncertainties of 0.15 for each contributing compound (NO and NO_2 for the NO_x OH reactivity, all 12 calibrated VOCs for the VOC OH reactivity).

References

Atkinson, R., Aschmann, S. M., Winer, A. M., and Pitts Jr., J. N.: Rate constants for the gas-phase reactions of O_3 with a series of carbonyls at 296 K, Int. J. Chem. Kinet., 13, 1133–1142, https://doi.org/10.1002/kin.550131104, 1981.

Atkinson, R., Carter, W. P. L., Plum, C. N., Winer, A. M., and Pitts Jr., J. N.: Kinetics of the gas-phase reactions of NO_3 radicals with a series of aromatics at 296 ± 2 K, Int. J. Chem. Kinet., 16, 887–898, https://doi.org/10.1002/kin.550160709, 1984.

Bohn, B. and Zetzsch, C.: Kinetics and mechanism of the reaction of OH with the trimethylbenzenes – experimental evidence for the formation of adduct isomers, Phys. Chem. Chem. Phys., 14, 13933–13948, https://doi.org/10.1039/C2CP42434G, 2012.

Carter, W. P. L.: Updated Maximum Incremental Reactivity Scale and Hydrocarbon Bin Reactivities for Regulatory Applications, Calif. Air Resour. Board Contract 2009, 339, 2009.

Duncianu, M., Olariu, R. I., Riffault, V., Visez, N., Tomas, A., and Coddeville, P.: Development of a New Flow Reactor for Kinetic Studies. Application to the Ozonolysis of a Series of Alkenes, J. Phys. Chem. A, 116, 6169–6179, https://doi.org/10.1021/jp211480x, 2012.

Gu, S., Guenther, A., and Faiola, C.: Effects of Anthropogenic and Biogenic Volatile Organic Compounds on Los Angeles Air Quality, Environ. Sci. Technol., 55, 12191–12201, https://doi.org/10.1021/acs.est.1c01481, 2021.

IUPAC: Evaluated Kinetic Data, International Union of Pure and Applied Chemistry (IUPAC) Task Group on Atmospheric Chemical Kinetic Data Evaluation [dataset], https://iupac.aeris-data.fr/, 2026.

Kramp, F. and Paulson, S. E.: On the Uncertainties in the Rate Coefficients for OH Reactions with Hydrocarbons, and the Rate Coefficients of the 1,3,5-Trimethylbenzene and m-Xylene Reactions with OH Radicals in the Gas Phase, J. Phys. Chem. A, 102, 2685–2690, https://doi.org/10.1021/jp973289o, 1998.

Ohta, T.: Rate constants for the reactions of OH radicals with alkyl substituted olefins, Int. J. Chem. Kinet., 16, 879–886, https://doi.org/10.1002/kin.550160708, 1984.

Pate, C. T., Atkinson, R., and Pitts Jr., J. N.: The gas phase reaction of O_3 with a series of aromatic hydrocarbons, J. Environ. Sci. Health Part Environ. Sci. Eng., 11, 1–10, https://doi.org/10.1080/10934527609385750, 1976.

Shaw, J. T., Rickard, A. R., Newland, M. J., and Dillon, T. J.: Rate coefficients for reactions of OH with aromatic and aliphatic volatile organic compounds determined by the multivariate relative rate technique, Atmos. Chem. Phys., 20, 9725–9736, https://doi.org/10.5194/acp-20-9725-2020, 2020.

Wu, R. and Xie, S.: Spatial Distribution of Secondary Organic Aerosol Formation Potential in China Derived from Speciated Anthropogenic Volatile Organic Compound Emissions, Environ. Sci. Technol., 52, 8146–8156, https://doi.org/10.1021/acs.est.8b01269, 2018.